

Superradiance in alpha clustered mirror nuclei

Alexander Volya^{1,2}, Marina Barbui¹, Vladilen Z. Goldberg² & Grigory V. Rogachev^{2,3,4}

Resonances in unstable quantum systems are radiating states that despite decaying overall normalization have a well-defined structure which is being balanced by outgoing radiation. Such an interplay between outgoing wave and internal quantum many-body dynamics leads to several unique effects. One of those is known as superradiance, or alignment, where due to decay or virtual coupling to the continuum the states undergo restructuring so that their wave functions align towards the decay channels thus facilitating the decay. This effect is well understood theoretically and is closely related to the fundamental properties of reaction physics. Direct observation of superradiance in open quantum many-body systems is difficult because it is hard to find identical complex quantum systems that are different only in their coupling to the continuum of reaction states describing the decay. Here we report this phenomenon in alpha cluster decays of mirror nuclei ^{18}O and ^{18}Ne .

¹ Department of Physics, Florida State University, Tallahassee 32306-4350, USA. ² Cyclotron Institute, Texas A&M University, College Station, TX 77843-3366, USA. ³ Department of Physics and Astronomy, Texas A&M University, College Station, TX 77843, USA. ⁴ Nuclear Solutions Institute, Texas A&M University, College Station, TX 77843, USA.  email: avolya@fsu.edu

The physics of open or unstable quantum many-body systems is at the frontier of modern science including broad areas such as quantum information science, mesoscopic physics, and biological systems. Atomic nuclei, being unique natural self-bound quantum systems that drastically vary in size and shape and exhibit phenomena covering quantum many-body physics, relativity, chaos, and physics beyond the standard model, offer a perfect arena for exploring the physics on the verge of stability. Recent advancements in experimental techniques using unstable radioactive beams and over a hundred years of development of theoretical methods position nuclear physics at the focal point.

The concept of an isolated quantum system is an idealization that becomes problematic for unstable systems or once we manipulate or carry out measurements. The dynamics of a relatively long-lived quasi-stationary state in the most physically relevant time interval is described by an exponential time-dependence in the wave function $\exp(-iEt - \Gamma t/2)$ that can be viewed as a complex energy state

$$\mathcal{E} = E - \frac{i}{2}\Gamma. \quad (1)$$

This exponential dynamics reflects the time evolution of the primary resonant component, the early-time evolution that depends on the structure of the initial state, and the late-time evolution once the principal resonant component decays are different¹⁻³.

Among many possible theoretical strategies the approach where the time evolution of an open system is described with an effective non-hermitian energy-dependent Hamiltonian operator $\mathcal{H}(E)$ is the most convenient one because it naturally extends the stationary state formalism used in many-body configuration interaction techniques. The matrix element of $\mathcal{H}(E)$ operator is written as

$$\mathcal{H}_{12}(E) = H_{12}(E) - \frac{i}{2} \sum_{c(\text{open})} A_1^c(E) A_2^{c*}(E), \quad (2)$$

where in similarity with the expression for the energy in Eq. (1), H represents the hermitian part, and the remaining non-hermitian part is given by energy-dependent channel vectors for each open decay channel c . The non-hermitian energy-dependent effective Hamiltonian (2) is a part of a many-body propagator and the resulting approach is formally exact and amounts to the Feshbach projection formalism⁴ that separates Hilbert space into internal and external subspaces. The method is closely connected to other strategies going back to old works⁵⁻⁸. The non-hermitian energy-dependent effective Hamiltonian approach is widely used in practice⁹⁻¹² as it provides a rather natural generalization of Eq. (1) and a good strategy for discussing the role of decay and its effects on the structure. In particular, when the decay is slow and thus the decay widths are small the non-hermitian part can be treated perturbatively. Starting from a stationary solution $H|\psi\rangle = E|\psi\rangle$ we recover Eq. (1) as

$$\mathcal{E} \approx \langle \psi | \mathcal{H} | \psi \rangle = E - \frac{i}{2} \sum_c \Gamma_c \text{ where } \Gamma_c = | \langle A^c | \psi \rangle |^2. \quad (3)$$

An interesting situation, referred to as superradiance, is expected in the opposite limit when the non-hermitian part becomes very large¹³. In that limit, due to the factorized nature of the Hamiltonian operator in Eq. (2) the structure of resonant states changes. Some states become more aligned along the dominant channels and thus become superradiant, while others decouple from the decay and become trapped. The term superradiance originates from the coherent radiation phenomenon by gas atoms coupled through a common radiation field¹⁴⁻¹⁶ is well

known in quantum optics and has been observed in some atomic systems, however, its manifestation in nuclear physics is not yet clear¹⁷.

The structural effects due to system being open and unstable are illusive because experimentally it is difficult to turn off the decay or provide an identical system with a different level of openness. In this work we use charge independence of nuclear forces, also referred to as isospin symmetry. While this symmetry is not exact, being primarily broken by the Coulomb interaction, it is of a perturbative nature. Except for some special cases such as near-degeneracy between levels, the isospin mixing in the wave functions is at the level of a few percent. This means that structurally the wave functions of the well-bound mirror systems are nearly identical. The coupling of mirror systems to decay channels can, however, be extremely different. Different decay energies, and differences in the coulomb barrier, lead to very different decay widths. Some structural differences are also expected in the direct vicinity of the thresholds.

Results and discussion

Illustrative model. Let us illustrate the superradiance mechanism using a simple two-level model^{18,19}, this model has been realized and studied experimentally, for example, using two interacting resonances in a microwave cavity²⁰. Consider two unperturbed levels with spacing ϵ that interact with the off-diagonal interaction ν and the upper level is coupled to a continuum, thus has a width Γ . The effective non-hermitian Hamiltonian for this system has a matrix form

$$H = \begin{pmatrix} \epsilon - \frac{i}{2}\Gamma & \nu \\ \nu & 0 \end{pmatrix} = H_0 - \frac{i\Gamma}{2} A^\dagger A, \quad \text{where } A = \begin{pmatrix} 1 \\ 0 \end{pmatrix}. \quad (4)$$

Here A is a channel vector. To simplify the model we assume that being relatively far from the thresholds the energy dependence is weak and the effective Hamiltonian does not change much in the energy region of interest.

For a stable system, when $\Gamma = 0$, we recover a textbook problem of a two-state system, where diagonalization gives energies of the two states as

$$E_{1,2} = \frac{1}{2} \left(\epsilon \pm \sqrt{\epsilon^2 + 4\nu^2} \right), \quad (5)$$

and their wave functions expressed in this basis as two-component eigenvectors. The spectroscopic factors (SF), determined by overlaps of eigenvectors with the channel vector, A are

$$SF_{1,2} = \frac{1}{2} \left(1 \pm \frac{\epsilon}{\sqrt{\epsilon^2 + 4\nu^2}} \right). \quad (6)$$

In the general case, when a decaying system is described by non-hermitian Hamiltonian in Eq. (4), the eigenvalues are complex corresponding to resonances and their widths. These complex energies are

$$\mathcal{E}_{1,2} = \frac{1}{2} \left(\epsilon - \frac{i}{2}\Gamma \pm \sqrt{\left(\epsilon - \frac{i}{2}\Gamma \right)^2 + 4\nu^2} \right). \quad (7)$$

The width of the states are $\Gamma_{1,2} = -2 \text{Im}(\mathcal{E}_{1,2})$, and the spectroscopic factors are still equal to the magnitude squared of overlaps of eigenvectors with the channel vector A . However, it can be shown that

$$SF_{1,2} = \Gamma_{1,2}/\Gamma. \quad (8)$$

This exact expression is very convenient in practice as it allows to determine spectroscopic factors based on observed widths and the total channel strength given by the width Γ .

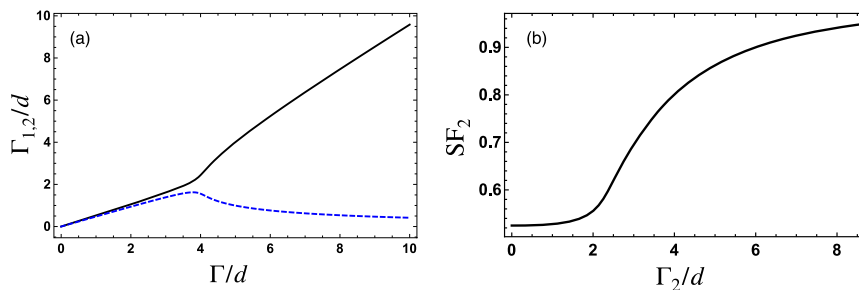


Fig. 1 Superradiance in the two-level model. **a** Widths of states in the two-level model as a function of continuum coupling Γ . The width of the superradiant state Γ_2 is shown by the solid black line, while the width of the continuum-decoupled state Γ_1 is shown with a blue dashed line. The parameters of the model $\epsilon = 0.1$ and $v = 1$. Energy scale is defined by the level spacing d . The effect of superradiance is in that one state absorbs all of the width, while the other state becomes trapped and its decay width goes to zero. **b** Spectroscopic factor of the superradiant state SF_2 as a function of its width Γ_2 . Sharp increase of the spectroscopic factor indicates a superradiant alignment.

It follows from Eq. (7) that as Γ increases and becomes very large, the superradiant state \mathcal{E}_2 (solution with a minus sign) absorbs all of the width, while the other state becomes decoupled from decay, having nearly zero width. In Fig. 1a we show the widths of the two states as a function of Γ .

The effect of structural alignment is highlighted by the changes in the SFs. Given our choice of parameters with nearly maximal level mixing (large v), initially, the two levels have nearly the same SFs and about the same width, but when Γ becomes large one state becomes superradiant. The SF of the superradiant state is shown in Fig. 1b as a function of its width Γ_2 ; as its width increases, implying stronger continuum coupling, the state aligns towards the decay channel and SF approaches the maximum allowed value of 1. This simple, yet fundamental, model also exemplifies the overlapping nature of resonances by relating level spacing $d = \sqrt{\epsilon^2 + 4v^2}$ to the cumulative width Γ of the channel. The transition to superradiance takes place when the real part of the expression under the square root in Eq. (7) becomes zero, at $\Gamma = 2d$, meaning that the resonances become overlapping. Because there are only two levels the superradiant state spectroscopic factor (the larger one) is always greater than 0.5, which of course is not the case in general.

Superradiance in ^{18}O and ^{18}Ne mirror nuclei. In realistic situations the coupling to continuum, modeled above by Γ , is primarily determined by the structure of the state in question and the kinematics of the decay channel defined by the decay energy, and Coulomb and centrifugal barriers (angular momentum). Assessing the role of continuum in atomic nuclei is difficult because there is no option of modifying the role of the continuum (continuum coupling) by changing, for example, the strength of Coulomb interaction or shifting the energy of the state in question with respect to the Coulomb or centrifugal barriers. In this sense, the structure of states in mirror nuclei provides a unique perspective on the effects of different continuum coupling. The wave functions for the analogous states in mirror nuclei are expected to be nearly identical in bound state approximation due to proton-neutron symmetry. On the other hand, coupling to the continuum may be very different as a result of different electric charges and energy above the respective decay threshold.

There are, of course, well-documented single particle differences related to continuum²¹, such as Nolen-Schiffer effect²². Recent observations of extreme proton-rich nuclei²³ address some similar phenomena. However, strongly continuum-coupled single-particle states often appear low in the spectrum where the density of states is low. Such resonances are well described by the particle plus potential model and are not intermixed with

many-body complexity. As a result, they do not allow for a good assessment of the continuum effects on many-body wave functions. On the other hand, single-particle strength in complex, compound resonances, is extremely weak to draw any conclusion about structural changes due to decay.

Clustering, being a many-body phenomenon, combined with isospin symmetry is a perfect arena to explore the effects of the continuum on the many-body structure. The connection between clustering, continuum, and decay thresholds has been highlighted long ago by Ikeda²⁴. In mirror nuclei, the threshold for the decay by alpha particles is different, therefore the observed widths of mirror alpha cluster resonances should differ because of different penetrability. The different widths should influence the interaction with the continuum, and we expect differences in the reduced widths (spectroscopic factors, preformation factors) of alpha cluster states in mirror nuclei. Moreover, due to many-body complexity, many channels with different angular momentum can be present which results in many strongly clustered states with different continuum coupling.

The development of rare isotope beam facilities propelled experimental studies of alpha cluster structures, including mirror nuclei^{25–27}. However, going away from the $N = Z$ line is more challenging as additional nucleonic degrees of freedom complicate the resonant spectrum and introduce new decay channels. Here we report on a single case that we were able to find which appears to be just right for this study. This is the case of $^{14}\text{C} + \alpha$ ²⁸ and $^{14}\text{O} + \alpha$ ²⁷ which allows to compare alpha resonances in mirror nuclei ^{18}O and ^{18}Ne . The α particle decay thresholds are 6.23 MeV in ^{18}O and 5.11 MeV in ^{18}Ne ; this and the difference in the Coulomb barrier results in the difference in penetrability factors. The levels with substantial reduced alpha width and thus well coupled to alpha channels were observed in both measurements^{27,28}. These resonances are selected for a comparative analysis in Table 1. For each pair of mirror states of a given spin-parity in ^{18}Ne and ^{18}O the table includes excitation energy, E_{ex} ; the observed total width Γ_{tot} ; and the partial width for the alpha channel Γ_{α} ; with the remaining width being predominantly in the single particle channel. The dimensionless reduced width, θ_{α}^2 , also listed in the table, represents the ratio of the α -reduced width obtained from the R-matrix fit for each resonance to the single particle limit (also called Wigner limit)^{27,29}. Following Eq. (8) we interpret it as the spectroscopic factor.

Comparative analysis of mirror data in Table 1 shows remarkable evidence of superradiance: the spectroscopic factors of mirror states are not equal and the states with larger alpha partial widths also tend to have larger spectroscopic factors and larger dimensional reduced widths. We emphasize, that given isospin symmetry, one would expect these quantities to be

Table 1 Mirror resonances in ^{18}Ne and ^{18}O .

^{18}Ne				^{18}O				
J^π	E_{ex} (MeV)	Γ_{tot} (keV)	Γ_α (keV)	θ_α^2	E_{ex} (MeV)	Γ_{tot} (keV)	Γ_α (keV)	θ_α^2
0 ⁺	9.8 (3)	4200	4200	1.4 (6)	9.9 (1)	3200	3200	1.9 (5)
1 ⁻	9.13 (2)	990	390	0.22 (2)	9.19 (2)	220	200	0.20 (1)
1 ⁻	9.61 (2)	1640	1120	0.52 (5)	9.76 (2)	700	630	0.46 (4)
1 ⁻	10.56 (4)	380	320	0.11 (5)	10.8 (3)	690	630	0.29 (4)
1 ⁻	13.73 (1)	1200	780	0.2 (1)	14.3 (3)	900	400	0.10 (4)
2 ⁺	9.21 (3)	540	270	0.21 (2)	9.79 (6)	170	90	0.10 (3)
2 ⁺	10.8 (1)	1580	1350	0.55 (3)	12.21 (8)	1100	1000	0.37 (9)
2 ⁺	13.4 (2)	1800	1750	0.45 (8)	12.8 (3)	4800	4800	1.56 (13)
3 ⁻	8.76 (8)	870	440	1.0 (4)	9.35 (2)	180	110	0.48 (13)
3 ⁻	11.0 (1)	1130	380	0.21 (7)	11.95 (1)	560	300	0.17 (2)
3 ⁻	12.7 (2)	2300	2000	0.7 (2)	12.98 (4)	1040	770	0.32 (5)
3 ⁻	14.8 (2)	5300	4000	1.0 (2)	14.0 (2)	2600	2100	0.7 (1)
4 ⁺	13.3 (3)	870	850	0.37 (4)	13.46 (2)	540	210	0.12 (1)
4 ⁺	14.15 (21)	620	380	0.14 (10)	14.77 (5)	680	680	0.28 (2)
5 ⁻	11.31 (4)	65	15	0.03 (2)	11.63 (1)	40	30	0.13 (1)
5 ⁻	12.9 (2)	670	530	0.48 (12)	13.08 (1)	180	120	0.17 (1)
5 ⁻	13.79 (8)	290	220	0.14 (10)	14.1 (1)	560	260	0.23 (2)
5 ⁻	14.6 (7)	1180	520	0.27 (20)	14.7 (1)	280	230	0.16 (6)
6 ⁺	11.8 (2)	260	40	0.23 (7)	11.69 (5)	23	12	0.23 (1)
6 ⁺	12.4 (2)	350	170	0.56 (26)	12.57 (1)	70	50	0.38 (8)

Summary of the resonance parameters observed in the elastic scattering of ^{14}O on α , ref. 27 and ^{14}C on α , ref. 28. E_{ex} is the excitation energy of the state, J^π indicates spin and parity, Γ_{tot} is the total width of the state, Γ_α is the partial alpha width, θ_α^2 is the alpha dimensionless reduced width. The particle thresholds for alpha emission are 5.112 MeV for ^{18}Ne and 6.227 MeV for ^{18}O .

roughly the same since they represent a structural overlap of the wave function with the channel, see Eqs. (6) and (8). The results suggest superradiance shown in Fig. 1b where SF increases with the width. Given the high excitation energy, the widths of these broad states are comparable with the level spacing; thus, the condition for superradiance is satisfied. The trapped states, being nearly decoupled from the alpha channels, are difficult to see in these experiments, however many states are known from other studies. The number of channels, which for each partial wave are differentiated by the number of nodes in the relative wave function, is known; and general location in the excitation spectrum and structure of the broad states, including which channels they are coupled to is relatively well understood theoretically from the quantum many-body configuration interaction calculations²⁷. The existing theory, which commonly relies on isospin symmetry, is not yet at the level of precision to give a quantitative assessment of the observed realignment effects due to decay.

The main feature of superradiance is that out of all states coupled to a given channel one absorbs most of the width and the other ones become trapped is seen in many alpha scattering experiments where broad states saturating the Wigner limit have been seen. Our study here makes a causal connection because stronger alignment is found in faster decaying nucleus of the two otherwise symmetric isospin partners.

In order to highlight the alignment effect associated with superradiance, in Fig. 2 for each pair of mirror states, we plot the ratio of spectroscopic factors as a function of the ratio of the partial alpha decay widths. If the spectroscopic factors of mirror states were the same then the ratio $\theta_\alpha^2(\text{Ne})/\theta_\alpha^2(\text{O}) = 1$, this is shown by the dashed line. Some deviations from unity can be expected, however Fig. 2 shows that the spectroscopic factors are correlated with the level of continuum coupling. Stronger continuum coupling (thus larger width) implies a larger spectroscopic factor; so that if $\Gamma_\alpha(\text{Ne})/\Gamma_\alpha(\text{O}) > 1$ then $\theta_\alpha^2(\text{Ne})/\theta_\alpha^2(\text{O}) > 1$, (area highlighted in red); and vice versa, weaker coupling implies smaller spectroscopic factor (area highlighted in blue). Despite the error bars and other limitations of the experiment, the

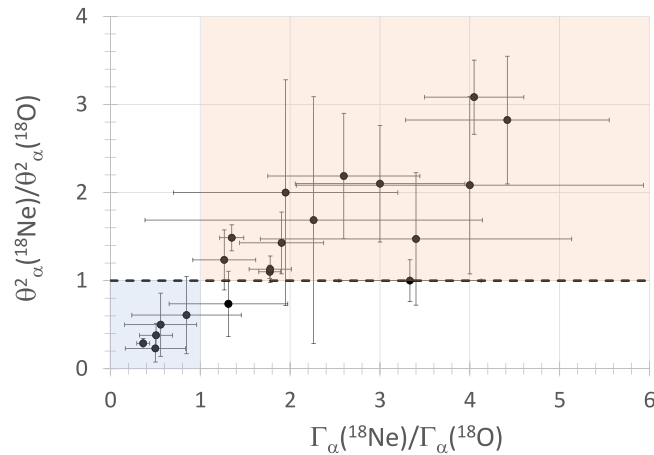


Fig. 2 Ratios of spectroscopic factors in mirror nuclei. For each pair of mirror states the ratio of spectroscopic factors $\theta_\alpha^2(\text{Ne})/\theta_\alpha^2(\text{O})$ is shown as a function of the ratio of the observed alpha decay widths $\Gamma_\alpha(\text{Ne})/\Gamma_\alpha(\text{O})$. The dashed line shows $\theta_\alpha^2(\text{Ne})/\theta_\alpha^2(\text{O})=1$; points in highlighted areas support superradiance. The error bars represent the uncertainties in the R-matrix fit parameters.

evidence for alignment is significant; out of 20 data points all, but one, which is a very broad 0^+ with large experimental uncertainties, follow this trend. The likelihood of this occurring by chance is small. This observation provides an interesting and exciting hint for the superradiance in nuclear systems. Of course, this observation should be scrutinized in future work. High statistics measurements and R-matrix analysis that directly includes other decay channels are necessary. It would also be interesting to use different reactions, such as alpha-transfer, to populate the cluster states and provide an independent measure of the total width and branching ratios in mirror nuclei to verify and benchmark current findings. Yet, our findings here may be the clearest manifestation of the superradiance phenomenon in nuclear physics to date.

Conclusion

Studies of alpha clustering in mirror nuclei is a promising new direction of research which among many benefits also allows to explore the physics of open quantum many-body systems and study how different decay rates reflected by the amplitude of the outgoing wave influences the structure of the resonating state. The first measurements of alpha clustering in mirror systems ^{18}O and ^{18}Ne reported in recent experiments^{27,28} provide evidence for superradiance where decaying states appear to gain additional alignment towards decay channels due to their decay. Future experiments and continuum shell model studies should allow for a more in-depth and quantitative understanding of the phenomenon.

Methods

Our findings are based on the results of two experiments^{27,28}. The Thick Target Inverse Kinematics technique (TTIK) was used to measure the excitation function for the $^{14}\text{C} + \alpha$ elastic scattering at the Florida State University, John D. Fox Superconducting Linear Accelerator facility. Though ^{14}C is radioactive ($T_{1/2} \approx 5300$ years), the long half-life gives a possibility to use the accumulated ^{14}C material for the acceleration, and the intensity of the ^{14}C beam was high. Therefore, the measurements²⁸ have good counting statistics. The energy resolution is conventional for the TTIK measurements (30 keV c.m. at large c.m. scattering angles but gradually deteriorating toward smaller c.m. angles). The excitation functions were analyzed using a multilevel, multichannel R-matrix code.

The $^{14}\text{O} + \alpha$ excitation measurements were performed at the radioactive beam facility (MARS) of the Cyclotron Institute at Texas A&M University³⁰ at ^{14}O beam intensity of 10^4 pps. The reaction $^{14}\text{O} + \alpha$ was also studied in inverse kinematics using the TexAT active target³¹. The TexAT active target allows to have the same energy resolution at all angles and separates elastic scattering from the inelastic one (the last was important because of a lower decay threshold in ^{18}Ne). The $^{14}\text{O} + \alpha$ excitation functions for elastic scattering were analyzed using the same R-matrix code as in work by Avila et al.²⁸ and the same channel radius was used in the fit. Data²⁶, where $^{14}\text{O} + \alpha$ resonance elastic scattering excitation function was measured at 180° in c.m., was also used in the fit.

The spectroscopic factor is assessed relative to the Wigner single particle decay width limit which is calculated as $\hbar^2/\mu a^2$, where μ is the reduced mass of the system and a is a channel radius. The Wigner limit is evaluated²⁷ assuming a channel radius of $a = 5.2$ fm following the phenomenological approach²⁹. The same channel radius is used in the R-matrix fits for both the ^{18}O and ^{18}Ne nuclei. Since coupling to the continuum is almost exclusively determined by barrier penetrability, the channel radius and the exact method of its evaluation do not change our discussion and conclusions.

Data availability

All data generated or analyzed during this study are included in this published article. The excitation functions for $^{14}\text{C} + \alpha$ and $^{14}\text{O} + \alpha$ resonance scattering and the raw data for the $^{14}\text{O} + \alpha$ experiment are available upon request.

Received: 3 August 2022; Accepted: 29 November 2022;

Published online: 10 December 2022

References

1. Baz, A. I., Zeldovich, I. B. & Perelomov, A. M. Scattering, reactions and decay in nonrelativistic quantum mechanics. (Rasseyanie, reaktsii i raspady v nerelyativistskoi kvantovoi mekhanike) (Israel Program for Scientific Translations, Jerusalem, 1969).
2. Fonda, L., Ghirardi, G. C. & Rimini, A. Decay theory of unstable quantum systems. *Rep. Prog. Phys.* **41**, 587–631 (1978).
3. Peshkin, M., Volya, A. & Zelevinsky, V. Non-exponential and oscillatory decays in quantum mechanics. *EPL* **107**, 40001 (2014).
4. Feshbach, H. A unified theory of nuclear reactions. *Ann. Phys.* **19**, 287 (1962).
5. Gamow, G. Zur quantentheorie des atomkernes. *Z. Phys.* **51**, 204 (1928).
6. Teichmann, T. Some general properties of nuclear reaction and scattering cross sections. *Phys. Rev.* **77**, 506 (1050).
7. Berggren, T. On the use of resonant states in eigenfunction expansions of scattering and reaction amplitudes. *Nucl. Phys.* **A109**, 265 (1968).
8. Fano, U. Effects of configuration interaction on intensities and phase shifts. *Phys. Rev.* **124**, 1866 (1961).
9. Volya, A. & Zelevinsky, V. Continuum shell model and nuclear physics at the edge of stability. *Phys. Nucl.* **77**, 969–982 (2014).
10. Volya, A. Time-dependent approach to the continuum shell model. *Phys. Rev. C* **79**, 044308 (2009).
11. Volya, A. & Zelevinsky, V. Continuum shell model. *Phys. Rev. C* **74**, 064314 (2006).
12. Volya, A. & Zelevinsky, V. Discrete and continuum spectra in the unified shell model approach. *Phys. Rev. Lett.* **94**, 052501 (2005).
13. Auerbach, N. & Zelevinsky, V. Super-radiant dynamics, doorways and resonances in nuclei and other open mesoscopic systems. *Rep. Prog. Phys.* **74**, 106301 (2011).
14. Kloc, M., Stránský, P. & Cejnar, P. Quantum quench dynamics in dicke superradiance models. *Phys. Rev. A* **98**, 013836 (2018).
15. Gross, M., Fabre, C., Pillet, P. & Haroche, S. Observation of near-infrared dicke superradiance on cascading transitions in atomic sodium. *Phys. Rev. Lett.* **36**, 1035 (1976).
16. Dicke, R. H. Coherence in spontaneous radiation processes. *Phys. Rev.* **93**, 99 (1954).
17. Kravvaris, K. & Volya, A. Quest for superradiance in atomic nuclei. *AIP Conf. Proc.* **1912**, 020010 (2017).
18. von Brentano, P. On the mixing of two bound and unbound levels: Energy repulsion and width attraction. *Phys. Rep.* **264**, 57 (1996).
19. Volya, A. & Zelevinsky, V. Non-hermitian effective hamiltonian and continuum shell model. *Phys. Rev. C* **67**, 054322 (2003).
20. Philipp, M., von Brentano, P., Pascovici, G. & Richter, A. Frequency and width crossing of two interacting resonances in a microwave cavity. *Phys. Rev. E* **62**, 1922 (2000).
21. Comay, E., Kelson, I. & Zidon, A. The thomas-ehrman shift across the proton dripline. *Phys. Lett. B* **210**, 31–34 (1988).
22. Nolen, J. A. & Schiffer, J. P. Coulomb energies. *Ann. Rev. Nucl. Sci.* **19**, 471–526 (1969).
23. Goldberg, V. Z. et al. First observation of 14f. *Phys. Lett. B* **692**, 307–311 (2010).
24. Ikeda, K., Tagikawa, N. & Horiuchi, H. The systematic structure-change into the molecule-like structures in the self-conjugate 4n nuclei. *Prog. Theo. Phys. Suppl.* **464** (1968).
25. Goldberg, V. Z. & Rogachev, G. V. α -cluster states in $n \neq z$ nuclei. *AIP Conf. Proc.* **1491**, 121–124 (2012).
26. Fu, C. et al. First observation of α -cluster states in the $^{14}\text{O} + ^4\text{He}$ interaction. *Phys. Rev. C* **77**, 064314 (2008).
27. Barbui, M. et al. α -cluster structure of ^{18}Ne . *Phys. Rev. C* **106**, 054310 (2022).
28. Avila, M. L. et al. alpha-cluster structure of o-18. *Phys. Rev. C* **90**, 024327 (2014).
29. Descouvemont, P. & Baye, D. The r -matrix theory. *Rep. Prog. Phys.* **73**, 036301 (2010).
30. Tribble, R. E., Burch, R. H. & Gagliardi, C. A. Mars: a momentum achromat recoil spectrometer. *Nucl. Instrum. Methods Phys. Res. A* **285**, 441–446 (1989).
31. Koshchiy, E. et al. Texas active target (texat) detector for experiments with rare isotope beams. *Nucl. Instrum. Methods Phys. Res. A* **957**, 163398 (2020).

Acknowledgements

This material is based upon work supported by the U.S. Department of Energy Office of Science, Office of Nuclear Physics under Award Number DE-SC0009883, and DE-FG02-93ER40773.

Author contributions

M.B., G.R., and V.G. carried all experimental work and analysis. A.V. was involved in theoretical interpretation, suggested the superradiance model and related evaluation of data. A.V. wrote the manuscript with significant input from all authors.

Competing interests

The authors declare no competing interests. G.R. is an Editorial Board Member for Communications Physics, but was not involved in the editorial review of, or the decision to publish this article.

Additional information

Correspondence and requests for materials should be addressed to Alexander Volya.

Peer review information Communications Physics thanks Yibin Qian and the other, anonymous, reviewer(s) for their contribution to the peer review of this work.

Reprints and permission information is available at <http://www.nature.com/reprints>

Publisher's note Springer Nature remains neutral with regard to jurisdictional claims in published maps and institutional affiliations.



Open Access This article is licensed under a Creative Commons Attribution 4.0 International License, which permits use, sharing, adaptation, distribution and reproduction in any medium or format, as long as you give appropriate credit to the original author(s) and the source, provide a link to the Creative Commons license, and indicate if changes were made. The images or other third party material in this article are included in the article's Creative Commons license, unless indicated otherwise in a credit line to the material. If material is not included in the article's Creative Commons license and your intended use is not permitted by statutory regulation or exceeds the permitted use, you will need to obtain permission directly from the copyright holder. To view a copy of this license, visit <http://creativecommons.org/licenses/by/4.0/>.

© The Author(s) 2022